J|A|C|S
ARTICLES
Published on Web 06/07/2006

Trehalose Click Polymers Inhibit Nanoparticle Aggregation and Promote pDNA Delivery in Serum

Sathya Srinivasachari, Yemin Liu, Guodong Zhang, Lisa Prevette, and Theresa M. Reineke*

Contribution from the the Department of Chemistry, University of Cincinnati, Cincinnati, Ohio 45221-0172

Received December 28, 2005; E-mail: Theresa.Reineke@uc.edu

Abstract: Herein, three new glycopolymers have been synthesized via "click polymerization" to promote nucleic acid delivery in the presence of biological media containing serum. These structures were designed to contain a trehalose moiety to promote biocompatibility, water solubility, and stability against aggregation, amide-triazole groups to enhance DNA binding affinity, and an oligoamine unit to facilitate DNA encapsulation, phosphate neutralization, and interactions with cell surfaces. A 2,3,4,2′,3′,4′-hexa-*O*-acetyl-6,6′-diazido-6,6′-dideoxy-D-trehalose (**4**) monomer was polymerized via copper(I)-catalyzed azide-alkyne cycloaddition with a series of dialkyne-amide comonomers that contain either one, two, or three Boc-protected secondary amines (**7a**, **7b**, or **7c**, respectively). After deprotection, three water-soluble polycations (**9a**, **9b**, or **9c**) were obtained with similar degrees of polymerization ($n = 56-61$) to elucidate the role of amine number on nucleic acid binding, complex formation, stability, and cellular delivery. Gel electrophoresis and ethidium bromide experiments showed that **9a**−**9c** associated with plasmid DNA (pDNA) and formed complexes (polyplexes) at N/P ratios dependent on the amine number. TEM experiments revealed that **9a**−**9c** polyplexes were small (50−120 nm) and had morphologies (spherical and rodlike) associated with the polymer chain stiffness. Dynamic light scattering studies in the presence of media containing serum demonstrated that **9c** polyplexes had a low degree of flocculation, whereas **9a** and **9b** polyplexesd aggregate rapidly. Further biological studies revealed that these structures were biocompatible and deliver pDNA into HeLa cells. Particularly, **9c** polyplexes promoted high delivery efficacy and gene expression profiles in the presence of serum.

Introduction

Synthetic materials are making a tremendous impact in many biomedical fields due to their potential to improve human health. In the emerging areas of drug and gene delivery,[1−5] tissue engineering,[6] and medical device design,[7] novel polymers are playing an important role in advancing these technologies. For instance, the study of noninvasive materials that bind with and compact nucleic acids into nanoparticles and effectively deliver exogenous genetic materials into cells is currently an area of intense interest. The extraordinary promise of oligonucleotide, siRNA, and genetic drugs to innovate therapeutic research and development has driven the rapid growth in this area.[2,5,8]

Creative chemical synthesis is central to develop innovative materials for specific biomedical applications. Indeed, subtle chemical and structural changes can have a profound impact on the biological properties;[4,9−11] therefore the synthetic methods and polymer structure must be carefully designed to be nontoxic

(1) (a) Davis, M. E.; Pun, S. H.; Bellocq, N. C.; Reineke, T. M.; Popielarski, S. R.; Mishra, S.; Heidel, J. D. *Curr. Med. Chem.* **2004**, *11*, 1241−1253. (b) Thomas, M.; Lu, J. J.; Ge, Q.; Zhang, C.; Chen, J.; Klibanov, A. M. *Proc. Natl. Acad. Sci. U.S.A.* **2005**, *102*, 5679−5684. (c) Pannier, A. K.; Shea, L. D. *Mol. Ther.* **2004**, *10*, 19−26. (d) Han, S.; Mahato, R. I.; Sung, Y. K.; Kim, S. W. *Mol. Ther.* **2000**, *2*, 302−317. (e) Zaric, V.; Weltin, D.; Erbacher, P.; Remy, J.-S.; Behr, J.-P.; Stephan, D. *J. Gene Med.* **2004**, *6*, 176−184.
(2) Davis, M. E. *Curr. Opin. Biotechnol.* **2002**, *13*, 128−131.
(3) Liu, Y.; Reineke, T. M. *J. Am. Chem. Soc.* **2005**, *127*, 3004−3015.
(4) Liu, Y.; Wenning, L.; Lynch, M.; Reineke, T. M. *J. Am. Chem. Soc.* **2004**, *126*, 7422−7423.
(5) Wagner, E. *Pharm. Res.* **2004**, *21*, 8−14.
(6) (a) Rydholm, A. E.; Bowman, C. N.; Anseth, K. S. *Biomaterials* **2005**, *26*, 4495−4506. (b) Wathier, M.; Jung, P. J.; Carnahan, M. A.; Kim, T.; Grinstaff, M. W. *J. Am. Chem. Soc.* **2004**, *126*, 12744−12745. (c) Hou, Q.; De Bank, P. A.; Shakesheff, K. M. *J. Mater. Chem.* **2004**, *14*, 1915−1923. (d) Zhang, R.; Tang, M.; Bowyer, A.; Eisenthal, R.; Hubble, J. *Biomaterials* **2005**, *26*, 4677−4683. (e) Hwang, J. J.; Iyer, S. N.; Li, L.-S.; Claussen, R.; Harrington, D. A.; Stupp, S. I. *Proc. Natl. Acad. Sci. U.S.A.* **2002**, *99*, 9662−9667.
(7) (a) Frost, M. C.; Reynolds, M. M.; Meyerhoff, M. E. *Biomaterials* **2005**, *26*, 1685−1693. (b) Langer, R.; Tirrell, D. A. *Nature* **2004**, *428*, 487−492.
(8) (a) Mann, M. J.; Dzau, V. J. *J. Clin. Invest.* **2000**, *106*, 1071−1075. (b) Tomita, N.; Azuma, H.; Kaneda, Y.; Ogihara, T.; Morishita, R. *Curr. Drug Targets* **2003**, *4*, 339−346. (c) Scherr, M.; Morgan, M. A.; Eder, M. *Curr. Med. Chem.* **2003**, *10*, 245−256. (d) Medema, R. H. *Biochem. J.* **2004**, *380*, 593−603. (e) Rubanyi, G. M. *Mol. Aspects Med.* **2001**, *22*, 113−142. (f) Nielsen, P. E. *Mol. Biotechnol.* **2004**, *26*, 233−248.
(9) (a) van de Wetering, P.; Moret, E. E.; Schuurmans-Nieuwenbroek, N. M. E.; Steenbergen, M. J. V.; Hennink, W. E. *Bioconjugate Chem.* **1999**, *10*, 589−597. (b) Hoggard, M. K.; Tubulekas, I.; Guan, H.; Edwards, K.; Nilsson, M.; Varum, K. M.; Artursson, P. *Gene Ther.* **2001**, *8*, 1108−1121. (c) Jones, N. A.; Hill, I. R. C.; Stolnik, S.; Bignotti, F.; Davis, S. S.; Garnett, M. C. *Biochim. Biophys. Acta* **2000**, *1517*, 1−18. (d) Malik, N.; Wiwattanapatapee, R.; Klopsch, R.; Lorenz, K.; Frey, H.; Weener, J. W.; Meijer, E. W.; Paulus, W.; Duncan, R. *J. Controlled Release* **2000**, *65*, 133−148. (e) Popielarski, S. R.; Mishra, S.; Davis, M. E. *Bioconjugate Chem.* **2003**, *14*, 672−678.
(10) Zelikin, A. N.; Putnam, D.; Shastri, P.; Langer, R.; Izumrudov, V. A. *Bioconjugate Chem.* **2002**, *13*, 548−553.
(11) (a) Wadhwa, M. S.; Collard, W. T.; Adami, R. C.; McKenzie, D. L.; Rice, K. G. *Bioconjugate Chem.* **1997**, *8*, 81−88. (b) Plank, C.; Tang, M. X.; Wolf, A. R.; Szoka, F. C. *Hum. Gene Ther.* **1999**, *10*, 319−332.

10.1021/ja0585580 CCC: $33.50

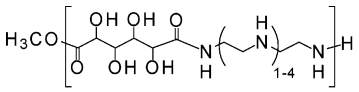

Figure 1. General structure of the poly(glycoamidoamine)s previously studied. The hydroxyl stereochemistry (D-glucose, *meso*-galactose, and D-mannose) and the amine stoichiometry were varied to yield a library of 12 structures.[3,4]

while remaining effective. To this end, devising new synthetic strategies that yield biocompatible polymers that are well-defined and chemically tailored to their specific function remains a significant challenge. In the fabrication of biomedical materials, the polymerization method plays a key role in the biological efficacy. For example, proteins are biologically synthesized polyamides; the cellular machinery can efficiently assemble and degrade amide linkages in a controlled manner, and for this reason, many synthetic polypeptide-based structures are being examined as biomaterials.[11,12] Polyesters are often utilized for drug and gene delivery because the hydrolyzable linkage facilitates controlled release of the drug and the resulting monomers and oligomers can be easily eliminated from biological systems.[13,14]

Particularly for genetic drug delivery, the polymeric vehicle should be designed to bind DNA strongly and compact nucleic acids into stable complexes (termed polyplexes) to facilitate effective cellular transport.[3,15,16] In a previous study, we have discovered that a seemingly insignificant modification in the repeat unit of poly(glycoamidoamine)s (shown in Figure 1), such as the stereochemistry of one hydroxyl group, can considerably increase the binding affinity to plasmid DNA (pDNA).[3] That study revealed that polymers that bind pDNA with higher affinity can improve cellular transport efficiency because they may help prevent dissociation caused by the concentrated salt environment, serum proteins, or anionic cell surface glycosaminoglycans that compete with polycation−DNA complexation. These harsh biological conditions can prematurely release and allow enzymatic degradation of the DNA before cellular uptake.

In the present study, we sought a new polymerization technique to synthesize polymers that would form exceptionally stable polyplexes to prevent dissociation in the presence of salt, serum, and cellular proteins. In addition, this reaction should serve to efficiently couple monomers containing disaccharides to promote the formation of higher molecular weight glycopolymers. Longer polymers may further stabilize polymer−DNA complexation through cooperative binding of the chemical groups to the DNA.[10,17,18] It was anticipated that a stronger binding affinity could reduce the amount of excess polymer needed to achieve high transfection efficiencies. High N/P ratios [the ratio of the secondary amines in the polymer (N)/phosphates (P) in pDNA] of 30 or more are often needed to observe elevated cellular delivery, which is acceptable for in vitro applications.[3,16,19] However, a large surplus of cationic material can cause polyplex aggregation in vivo and be rapidly cleared from circulation by the reticuloendothelial system.[2,5,14,20−22] These problems can prohibit drug delivery to the site of disease and cause severe toxicity and inflammation problems.

To design such materials, we were inspired by the works of Dervan et al., who have shown that macromolecules constructed with a motif containing various heterocyclic residues, such as derivatives of pyrrole and imidizole (H-bond acceptors) or *N*-methyl-3-hydroxypyrrole and hydroxybenzimidazole (H-bond donors), which are structurally adjacent to amides (H-bond donors), bind with nucleic acids in a remarkably specific and stable manner.[23] The complexation of these oligomers with the minor groove of DNA is driven by the strong hydrogen bonding of these groups with specific DNA base pairs that facilitate interactions similar to DNA-binding proteins. Huisgen cycloaddition, commonly known as the "click reaction", was an ideal transformation to form similar heterocycles during polymerization to improve the polymer−DNA binding stability by providing groups that could act as H-bond acceptors and increase hydrophobic interactions of these polymers with DNA.[24,25] In addition, this efficient reaction would serve to enhance the polymerization degree over previously studied monosaccharide-containing polyamides. The click reaction has been successfully applied to synthesize a variety of materials such as dendrimers,[26] dendronized linear polymers,[27] and adhesives[28] and has been particularly useful for molecular grafting onto polymers,[29]

(12) (a) Benns, J. M.; Choi, J.-S.; Mahato, R. I.; Park, J.-S.; Kim, S. W. *Bioconjugate Chem.* **2000**, *11*, 637−645. (b) Hisayasu, S.; Miyauchi, M.; Akiyama, K.; Gotoh, T.; Satoh, S.; Shimada, T. *Gene Ther.* **1999**, *6*, 689−693. (c) Park, Y.; Kwok, K. Y.; Boukarim, C.; Rice, K. G. *Bioconjugate Chem.* **2002**, *13*, 232−239. (d) Singh, D.; Bisland, S. K.; Kawamura, K.; Gariepy, J. *Bioconjugate Chem.* **1999**, *10*, 745−754. (e) Metzke, M.; O'Connor, N.; Maiti, S.; Nelson, E.; Guan, Z. *Angew. Chem. Int. Ed.* **2005**, *44*, 6529−6533.
(13) (a) Akinc, A.; Lynn, D. M.; Anderson, D. G.; Langer, R. *J. Am. Chem. Soc.* **2003**, *125*, 5316−5323. (b) Anastasiou, T. J.; Uhrich, K. E. *J. Polym. Sci. A: Polym. Chem.* **2003**, *41*, 3667−3679. (c) Padilla De Jesus, O. L.; Ihre, H. R.; Gagne, L.; Frechet, J. M.; Szoka, F. C. *Bioconjugate Chem.* **2002**, *13*, 453−461. (d) Ihre, H. R.; Padilla De Jesus, O. L.; Szoka, F. C.; Frechet, J. M. *Bioconjugate Chem.* **2002**, *13*, 443−452.
(14) Duncan, R. *Nat. Rev. Drug Discovery* **2003**, *2*, 347−360.
(15) (a) Kostiainen, M. A.; Hardy, J. G.; Smith, D. K. *Angew. Chem., Int. Ed.* **2005**, *44*, 2556−2559. (b) Rungsardthong, U.; Ehtezazi, T.; Bailey, L.; Armes, S. P.; Garnett, M. C.; Stolnik, S. *Biomacromolecules* **2003**, *4*, 683−690. (c) Chen, D. J.; Majors, B. S.; Zelikin, A. N.; Putnam, D. *J. Controlled Release* **2005**, *103*, 273−283.
(16) Liu, Y.; Reineke, T. M. *Bioconjugate Chem.* **2006**, *17*, 101−108.
(17) (a) Godbey, W. T.; Wu, K. K.; Mikos, A. G. *J. Biomed. Mater. Res.* **1999**, *45*, 268−275. (b) Sato, T.; Ishii, T.; Okahata, Y. *Biomaterials* **2001**, *22*, 2075−2080.
(18) Jonsson, M.; Linse, P. *J. Chem. Phys.* **2001**, *115*, 3406−3418.
(19) (a) Yang, T.-F.; Chin, W.-K.; Cherng, J.-Y.; Shau, M.-D. *Biomacromolecules* **2004**, *5*, 1926−1932. (b) Banerjee, P.; Reichardt, W.; Weissleder, R.; Bogdanov, A. *Bioconjugate Chem.* **2004**, *15*, 960−968. (c) Cryan, S.-A.; Holohan, A.; Donohue, R.; Darcy, R.; O'Driscoll, C. M. *Eur. J. Pharm. Sci.* **2004**, *21*, 625−633. (d) Hwang, S. J.; Bellocq, N. C.; Davis, M. E. *Bioconjugate Chem.* **2001**, *12*, 280−290.
(20) Roberts, M. J.; Bentley, M. D.; Harris, J. M. *Adv. Drug Delivery Rev.* **2002**, *54*, 459−476.
(21) (a) Storm, G.; Belliot, S. O.; Daemen, T.; Lasic, D. D. *Adv. Drug Delivery Rev.* **1995**, *17*, 31−48. (b) Hwang, S. J.; Davis, M. E. *Curr. Opin. Mol. Ther.* **2001**, *3*, 183−191.
(22) Kaneda, *Curr. Mol. Med.* **2001**, *1*, 493−499.
(23) (a) Dervan, P. B.; Edelson, B. S. *Curr. Opin. Struct. Biol.* **2003**, *13*, 284−299. (b) White, S.; Szewczyk, J. W.; Turner, J. M.; Baird, E. E.; Dervan, P. B. *Nature* **1998**, *391*, 468−471. (c) Best, T. P.; Edelson, B. S.; Nickols, N. G.; Dervan, P. B. *Proc. Natl. Acad. Sci. U.S.A.* **2003**, *100*, 12063−12068. (d) Fechter, E. J.; Dervan, P. B. *J. Am. Chem. Soc.* **2003**, *125*, 8476−8485.
(24) Rostovtsev, V. V.; Green, L. G.; Fokin, V. V.; Sharpless, K. B. *Angew. Chem., Int. Ed.* **2002**, *41*, 2596−2599.
(25) (a) Kolb, H. C.; Finn, M. G.; Sharpless, K. B. *Angew. Chem., Int. Ed.* **2001**, *40*, 2004−2021. (b) Perez-Balderas, F.; Ortega-Munoz, M.; Morales-Sanfrutos, J.; Hernandez-Mateo, F.; Calvo-Flores, F. G.; Calvo-Asin, J. A.; Isac-Garcia, J.; Santoyo-Gonzales, F. *Org. Lett.* **2003**, *5*, 1951−1954.
(26) (a) Wu, P.; Feldman, A. K.; Nugent, A. K.; Hawker, C. J.; Scheel, A.; Voit, B.; Pyun, J.; Frechet, J. M.; Sharpless, K. B.; Fokin, V. V. *Angew. Chem., Int. Ed.* **2004**, *43*, 3928−3932. (b) Malkoch, M.; Schleicher, K.; Drockenmuller, E.; Hawker, C. J.; Russell, T. P.; Wu, P.; Fokin, V. V. *Macromolecules* **2005**, *38*, 3663−3678.
(27) Helms, B.; Mynar, J. L.; Hawker, C. J.; Frechet, J. M. *J. Am. Chem. Soc.* **2004**, *126*, 15020−15021.
(28) Diaz, D. D.; Punna, S.; Holzer, P.; McPherson, A. K.; Sharpless, K. B.; Fokin, V. V.; Finn, M. G. *J. Polym. Sci. A: Polym. Chem.* **2004**, *42*, 4392−4403.
(29) Parrish, B.; Breitenkamp, R. B.; Emrick, T. *J. Am. Chem. Soc.* **2005**, *127*, 7404−7410.

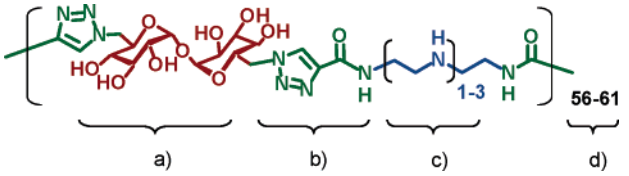

Figure 2. The target structures were designed to have unique features for stable DNA nanoparticle formation and enhanced nucleic acid delivery in the presence of serum: (a) a trehalose unit for increased biocompatibility, solubility, and stability in biological media containing serum, (b) heterocycle-amide groups (two per repeat unit) for hydrophobic, van der Waals, and H-bonding interactions with nucleic acids, (c) an oligoamine for electrostatic DNA binding, phosphate charge neutralization, and cellular uptake, and (d) higher degrees of polymerization to promote cooperative binding with DNA.

carbohydrate arrays,[30] bacteria,[31] viruses,[32] and living cells.[33] However, it has not been previously utilized to design glycopolymer nucleic acid delivery vehicles.

In this report, copper-catalyzed azide-alkyne cycloaddition has been exploited in the formation of a new family of glycopolymers (Figure 2). These structures have been chemically tailored to be nontoxic yet promote very stable nucleic acid complexation and prevent aggregation of polyplexes with biological proteins. Here, the synthesis of a disaccharide comonomer (Scheme 1), diazido-trehalose, is presented. This structure will ensure the biocompatibility and water solubility of the final polymers containing the aromatic triazoles. Trehalose is known for its unique properties as a cryo- and lyo-protectant, as it prevents aggregation, fusion, and lysis of lipid membranes and proteins.[34,35] This unusual property of trehalose has been attributed to its exceptionally large hydrated volume and the ability of this carbohydrate to modify the solvation layer around various biomolecules. We took advantage of this characteristic to reduce polyplex aggregation with serum proteins, which are known to significantly reduce cellular delivery.[2,36] Also, novel dialkyne-oligoamine monomers containing 1, 2, and 3 secondary amines were designed (Scheme 2) to facilitate DNA encapsulation and polyanion (DNA) neutralization and encourage cell surface interactions of the polyplexes with negatively charged glycosaminoglycans.[3,4,16,37] We incorporated triazole groups adjacent to the amides through click polymerization of the diazido-trehalose comonomer with the series of dialkyne-oligoamines as shown in Scheme 3. This repeated amide-heterocycle motif was developed to promote strong polycation−nucleic acid complexation via van der Waals, hydrophobic, and H-bonding interactions.[23] Last, the higher degrees of polymerization resulting from the facile click reaction will aid in stable polyplex formation via cooperative binding of the polymer with DNA.[10,17]

We discovered through ethidium bromide exclusion assays and dynamic light scattering studies that the presence of these functional groups promoted the formation of polyplexes that are stable in the presence of media containing 10% serum and physiological salt concentrations. It has been found that the length of the oligoamine unit affects the serum stability and biocompatibility of the polyplexes. Also, cellular uptake and luciferase reporter gene studies completed in both the absence and presence of serum revealed high gene delivery efficiency that was highly dependent on the number of secondary amines. This is the first study demonstrating that click polymerization is a highly effective means of forming biocompatible glycopolymers for biomedical applications, particularly for the cellular delivery of nucleic acids.

Results and Discussion

Synthesis and Characterization of Monomers and Polymers. As shown in Scheme 1, the disaccharide monomer 2,3,4,2′,3′,4′-hexa-*O*-acetyl-6,6′-diazido-6,6′-dideoxy-D-trehalose (**4**) was generated in three steps according to a combination of reported methods and was purified via recrystallization from methanol.[38] The novel series of dialkyne-oligoamine monomers (**7a**−**7c**, Scheme 2) were synthesized by first selectively protecting the primary amine end groups of diethylenetriamine, triethylenetetramine, and tetraethylenepentamine with trifluoroacetyl units ($COCF_3$) and the internal secondary amines with *tert*-butoxycarbonyl (Boc) according to a previously published method.[39] The terminal $COCF_3$ moieties were then cleaved with potassium carbonate, and the primary amines were coupled to propiolic acid via DCC (dicyclohexyl carbodiimide) coupling. The resulting new dialkyne monomers were purified via silica gel flash chromatography and the proper fractions isolated to yield **7a**−**7c** with the desired alkyne and amide functionalities.

As shown in Scheme 3, monomers **4** and either **7a**, **7b**, or **7c** were coupled in equal molar ratios via "click polymerization" according to a similar method exploited by Sharpless et al. for molecular coupling through a triazole linkage.[24,28] In brief, the monomers were polymerized in a 1:1 solution of *tert*-butyl alcohol and water containing copper(II) sulfate pentahydrate and sodium ascorbate as the catalyst at 50 °C to yield polymers of similar degrees of polymerization ($n = 56-61$, shown in Table 1). This was important to elucidate the effects of varying the amine number between the trehalose moieties without the results being affected by differences in molecular weight. After polymerization, the protected products (**8a**−**8c**) were isolated and characterized.

To yield the final water-soluble polymers, conventional deprotection chemistry was applied; the acetyl groups (OAc) were cleaved with sodium methoxide in methanol and the Boc groups deprotected with trifluoroacetic acid in dichloromethane. The final products (**9a**−**9c**, Scheme 3) were purified via exhaustive dialysis in ultrapure water, lyophilized, and analyzed for complete deprotection and molecular weight. According to NMR analysis, the OAc and Boc protecting groups were completely cleaved from the polymer backbone, as indicated

(30) Fazio, F.; Bryan, M. C.; Blixt, O.; Paulson, J. C.; Wong, C.-H. *J. Am. Chem. Soc.* **2002**, *124*, 14397−14402.
(31) (a) Link, A. J.; Tirrell, D. A. *J. Am. Chem. Soc.* **2003**, *125*, 11164−11165. (b) Link, A. J.; Vink, M. K. S.; Tirrell, D. A. *J. Am. Chem. Soc.* **2004**, *126*, 10598−10602.
(32) Wang, Q.; Chan, T. R.; Hilgraf, R.; Fokin, V. V.; Sharpless, K. B.; Finn, M. G. *J. Am. Chem. Soc.* **2003**, *125*, 3192−3193.
(33) Agard, N. J.; Prescher, J. A.; Bertozzi, C. R. *J. Am. Chem. Soc.* **2004**, *126*, 15046−15047.
(34) (a) Crowe, J. H.; Crowe, L. M. *Science* **1984**, *17*, 701−703. (b) Sola-Penna, M.; Meyer-Fernandes, J. R. *Arch. Biochem. Biophys.* **1998**, *360*, 10−14. (c) Lins, R. D.; Pereira, C. S.; Hunenberger, P. H. *Proteins* **2004**, *55*, 177−186.
(35) Engelsen, S. B.; Perez, S. *J. Phys. Chem. B* **2000**, *104*, 9301−9311.
(36) Leong, K. W. *MRS Bull.* **2005**, *30*, 640−646.
(37) Godbey, W. T.; Wu, K. K.; Mikos, A. G. *Proc. Natl. Acad. Sci. U.S.A.* **1999**, *96*, 5177−5181.
(38) (a) Reineke, T. M.; Davis, M. E. *Bioconjugate Chem.* **2003**, *14*, 247−254. (b) Garcia Fernandez, J. M.; Mellet, C. O.; Blanco, J. L. J.; Mota, J. F.; Gadelle, A.; Coste-Sarguet, A.; Defaye, J. *Carbohydr. Res.* **1995**, *268*, 57−71. (c) Menger, F. M.; Mbadugha, B. N. A. *J. Am. Chem. Soc.* **2001**, *123*, 875−885.
(39) Koscova, S.; Budesinsky, M.; Hodacova, J. *Collect. Czech. Chem. Commun.* **2003**, *68*, 744−750.

Scheme 1. Synthesis of the Diazido-Trehalose Comonomer[a]

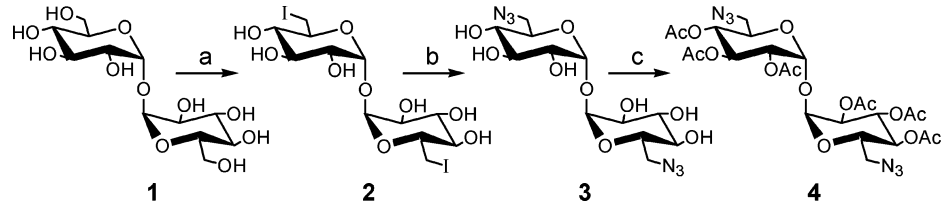

[a] Conditions: (a) PPh_3, I_2, DMF; (b) NaN_3, DMF; (c) 1:1 Ac_2O Pyr.

Scheme 2. Synthesis of the Dialkyne Comonomers[a]

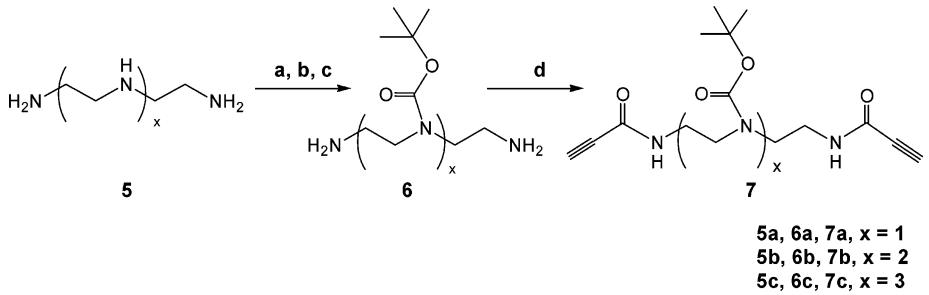

5a, 6a, 7a, x = 1
5b, 6b, 7b, x = 2
5c, 6c, 7c, x = 3

[a] Conditions: (a) CF_3COOEt, CH_2Cl_2; (b) $(Boc)_2O$, CH_2Cl_2, TEA; (c) K_2CO_3, 20:1 MeOH/H_2O; (d) propiolic acid, DCC, CH_2Cl_2.

Scheme 3. Click Polymerization and Polymer Deprotection[a]

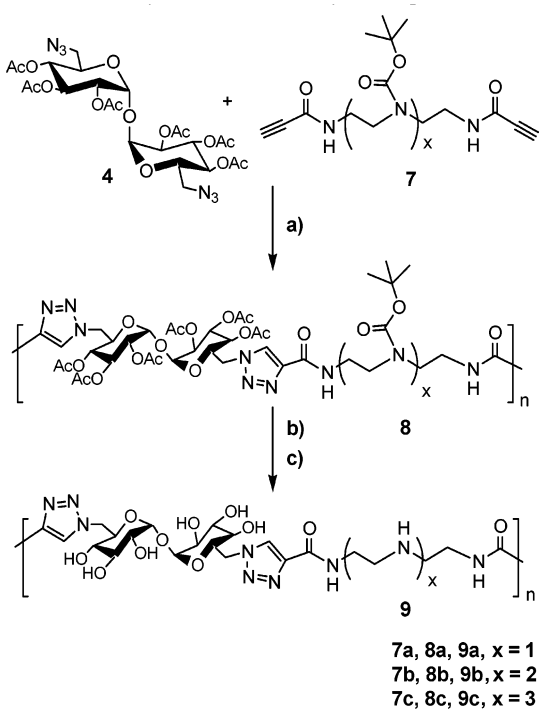

7a, 8a, 9a, x = 1
7b, 8b, 9b, x = 2
7c, 8c, 9c, x = 3

[a] Conditions: (a) $CuSO_4$/sodium ascorbate, 1:1 t-BuOH/H_2O; (b) NaOMe/MeOH; (c) CF_3COOH/CH_2Cl_2.

Table 1. MHS Parameter (α), Weight-Averaged Molecular Weight (M_w), Polydispersity (M_w/M_n), and Weight-Averaged Degree of Polymerization (n_w) for the Final Click Glycopolymers

polymer	MHS α	M_w (kDa)	M_w/M_n	n_w
9a	0.55	34	1.3	56
9b	0.74	39	1.2	61
9c	0.62	40	1.2	59

by the absence of peaks at 1.97−2.02 ppm (OAc) and 1.40 ppm (Boc). The deprotected polymers were also analyzed via GPC containing a triple detection system (refractive index, static light scattering, viscometry) to determine the molecular weight and viscosity of these systems. As shown in Table 1, polymers **9a**, **9b**, and **9c** were all successfully synthesized with similar degrees of polymerization to elucidate the effect of the number of ethyleneamine groups on the polymer−DNA binding affinity, polyplex stability, and cellular delivery efficacy. Viscosity measurements revealed that the polymers had slightly different Mark−Houwink−Sakurada (MHS) α values. This value is calculated from the MHS equation ($[\eta] = KM_v^{\alpha}$) by plotting the logarithm of the intrinsic viscosity versus the logarithm of the viscosity-averaged molecular weight distribution. The slope of the resulting line (α) provides a general indication of the polymer chain stiffness in solution (values of 0.5−0.8 indicate randomly coiled linear polymers, and values of 0.8−1.0 indicate stiffer chain structures). It was noticed that polymer **9b** had a slightly higher MHS α value (0.74), indicating that this particular polymer may have a slightly stiffer characteristic in aqueous media.

Polymer−pDNA Binding and Polyplex Stability. After synthesis and purification of the final deprotected polycations, **9a**−**9c** were examined for their ability to bind and charge-neutralize DNA using a gel electrophoretic shift assay. Each polymer was combined with pDNA at various N/P ratios between 0 and 15, loaded into the gel, and electrophoresed. It should be noted that only the secondary amines in the oligoamine unit were counted in calculating the N/P ratio, because we do not expect the amide and triazole nitrogens to be protonated at physiological pH due to their low pK_a values.[40] Figure 3a reveals that **9a** binds and neutralizes pDNA at N/P = 1.5, which is shown by the lack of pDNA migration at the N/P ratios of binding. Figure 3c (line) shows the N/P ratios of pDNA complexation and charge neutralization (gel shift) for **9a**−**9c**. All of the polymers stably associate and neutralize pDNA at low N/P values between 1.0 and 1.5, where **9c** revealed the lowest N/P ratio of binding (at N/P = 1.0) in the gel shift assay. When these results were compared to the poly(glycoamidoamine) gel shift assays previously reported,[3] it was noticed

(40) (a) Jencks, W. P.; Regenstein, J. *Handbook of Biochemistry and Molecular Biology: Physical and Chemical Data*, 3rd ed.; Fasman, G. D., Ed.; CRC Press: Cleveland, 1975; Vol. 1, p 345. (b) Catalan, J.; Abboud, J. L. M.; Elguero, J. In *Advances in Heterocyclic Chemistry*; Katritzky, A. R., Ed.; Academic Press: Orlando, FL, 1987; Vol. 41, pp 187−274.

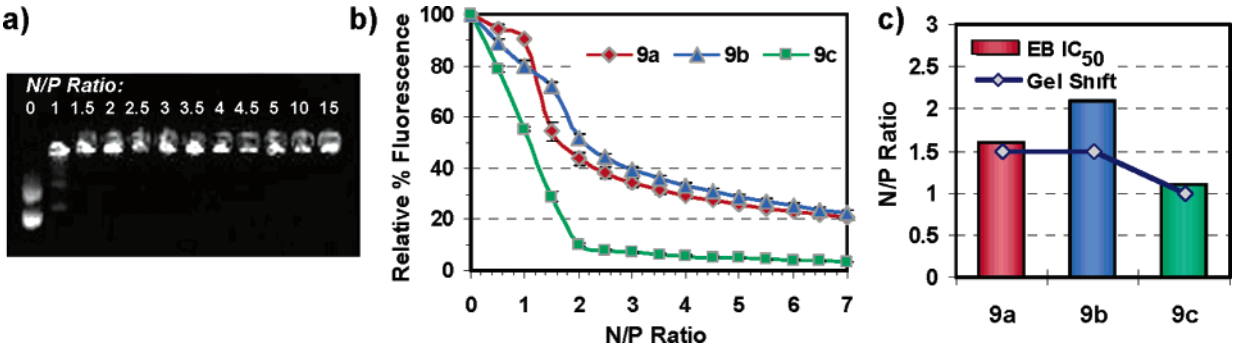

Figure 3. (a) Agarose gel electrophoretic pDNA-binding shift assay for glycopolymer **9a** at N/P ratios between 0 and 15 (determines the N/P ratio of pDNA charge neutralization). (b) Complexation of pDNA and polymers **9a**, **9b**, and **9c** at N/P ratios between 0 and 7 as monitored by EB exclusion. The results are reported as the relative percent of EB fluorescence, where 100% intensity is at N/P = 0 (EB + DNA only). (c) N/P ratios of glycopolymer−pDNA complexation. The line represents the N/P ratio of pDNA retardation as determined by gel shift assays. The bars represent the polymer amount (expressed as N/P ratio) that is needed for 50% EB exclusion from pDNA (IC_{50} value).

that the polymers with a low nitrogen density, **9a** and **9b**, bound pDNA at significantly lower N/P ratios (N/P = 1.5) than their poly(glycoamidoamine) analogues that do not contain repeated triazole groups (these analogues bound pDNA at N/P ratios between 2 and 5). This indicates that the repeated triazole-amide motif and/or the increased molecular weights of the click glycopolymers promote stronger DNA-binding affinity. In support of this finding, others have shown that polyamides containing aromatic heterocycles bind DNA in a highly stable manner, and the configuration and spacing of heterocycles, such as pyrrole and imidizole, affect binding affinity and specificity.[23,41] Also, Hergenrother et al. have shown that deoxystreptamine dimers linked by triazoles to a variety of bridging groups recognize and bind RNA hairpin loops with high affinity.[41] Last, theoretical[18] and experimental[42] studies have shown that increasing the length of polyelectrolytes tends to increase their capacity to complex oppositely charged macroions (such as DNA).

To further study the pDNA-binding characteristics of the trehalose click polymers, we completed ethidium bromide (EB) exclusion assays, which allow the relative pDNA affinity to be determined for these polymers. In this assay, the fluorescence of EB is significantly enhanced upon DNA intercalation. When a polymer binds DNA, EB is displaced from DNA and a reduction in fluorescence is observed (this effect is shown in Figure 3b). The results are typically reported as an IC_{50} value, which is the polymer amount (expressed as the polymer−DNA N/P ratio) required to produce 50% inhibition of EB fluorescence (a low IC_{50} value denotes strong binding).[43] For each polymer, the inhibitory concentration value (IC_{50} given as the N/P ratio) was determined to compare the effect of amine number (between 1 and 3; **9a**−**9c**) on the pDNA-binding affinity. As shown in Figure 3b and 3c (bars), polymer **9c** clearly had the highest binding affinity, as it revealed the lowest IC_{50} value of 1.1. Polymer **9a** yielded a higher IC_{50} value of 1.6, and **9b** displayed the highest IC_{50} value of 2.1 (weakest ability to exclude EB from pDNA). These results suggest that the number of amines and spacing of the triazole moieties along the polymer backbone clearly affects the binding affinity, where polymer **9c** associates with pDNA with the highest affinity and **9b** binds pDNA with the lowest affinity. This finding may be related to the polymer chain stiffness. Polymers **9a** and **9c** revealed lower MHS α values, indicating random coil solution structures; conversely, **9b** was found to have a higher MHS α value, indicating a stiffer chain solution structure. Several groups have reported that polymer chain stiffness significantly affects polycation−polyanion interactions.[44,45] The sharp bending of stiffer chain polymers (occurs upon DNA binding and compaction) is energetically unfavorable. If an extended chain structure is favored in aqueous solution, the formation of compact globular morphologies during polyplex assembly will be hindered.

Transmission electron microscopy was performed to directly observe the morphology of the formed polyplexes as a function of polymer structure. Polyplex formation is largely influenced by a complex combination of several factors such as chain stiffness and electrostatic and hydrogen-bonding interactions. Figure 4 shows TEM images of the polyplexes formed by complexing pDNA with polymers **9a**, **9b**, and **9c** at an N/P ratio of 7. It was noticed that polymers **9a** and **9b** formed polyplexes that ranged in size from about 80−125 nm and had spherical and rodlike morphologies, while **9c** formed smaller and mostly spherical polyplexes (50−100 nm). More rod-shaped complexes were found in the image of the **9b** polyplexes, which is likely related to the stiffer chain characteristic (α = 0.74) in aqueous solution than **9a** (α = 0.55) and **9c** (α = 0.62).[44]

Dynamic light scattering experiments were completed to examine the behavior and stability of the polyplexes in cell culture media containing physiological salt and 10% serum conditions. In water, polymers **9a**−**9c** assemble with and compact pDNA into polyplexes with an average hydrodynamic diameter between 91 and 172 nm (Figure 5). Zeta potential measurements of these systems in water revealed that all of the polyplexes had a high surface charge over 40 mV at an N/P = 7 (data now shown). When cell culture media (serum-free Opti-MEM or DMEM containing 10% fetal bovine serum) was added to the aqueous polyplex solutions, a dramatic difference in the

(41) Thomas, J. R.; Liu, X.-C.; Hergenrother, P. J. *J. Am. Chem. Soc.* **2005**, *127*, 12434−12435.
(42) Zelikin, A. N.; Trukhanova, E. S.; Putnam, D.; Izumrudov, V. A.; Litmanovich, A. A. *J. Am. Chem. Soc.* **2003**, *125*, 13693−13699.
(43) Read, M. L.; Bettinger, T.; Oupicky, D. In *Nonviral Vectors for Gene Therapy*; Findeis, M. A., Ed.; Humana Press: Totowa, NJ, 2001; Vol. 65, pp 131−148.
(44) (a) Maurstad, G.; Danielsen, S.; Stokke, B. T. *J. Phys. Chem. B* **2003**, *107*, 8172−8180. (b) Danielsen, S.; Maurstad, G.; Stokke, B. T. *Biopolymers* **2005**, *77*, 86−97.
(45) Kayitmazer, A. B.; Seyrek, E.; Dubin, P. L.; Staggemeier, B. A. *J. Phys. Chem. B* **2003**, *107*, 8158−8165.

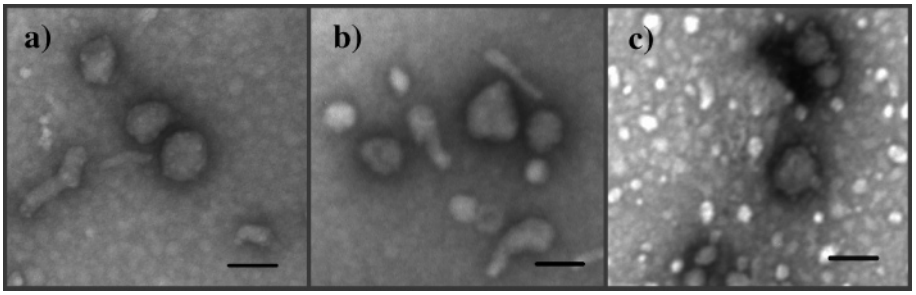

Figure 4. TEM images of polyplexes formed by complexing pDNA with polymers (a) **9a**, (b) **9b**, and (c) **9c**. The black bar in each image represents 100 nm.

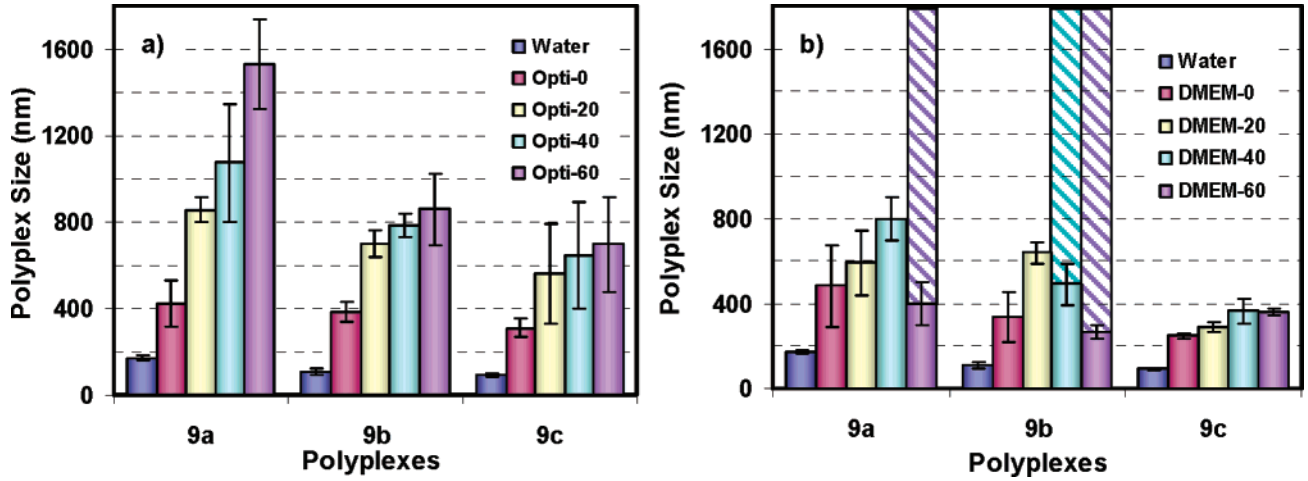

Figure 5. Dynamic light scattering studies of **9a**, **9b**, and **9c** polyplexes (N/P = 7). (a) The bars represent the polyplex sizes upon initial formulation in water and then 0, 20, 40, and 60 min after the addition of Opti-MEM (without serum). (b) The bars represent the polyplex sizes upon initial formulation in water and then 0, 20, 40, and 60 min after the addition of DMEM (with 10% serum). The dashed bars represent the presence of a bimodal distribution that included large aggregates greater than 3 μm.

polyplex stability was observed. As shown in Figure 5a, when Opti-MEM was added to the water solutions, rapid polyplex aggregation occurred due to neutralization of the surface charge with counterions. After exposure to this high salt condition for 60 min, polyplexes formed with **9a** aggregated to about 1500 nm, **9b** to 850 nm, and **9c** to 700 nm. When DMEM containing 10% serum was introduced into the polyplex solutions, a drastically different trend was observed. As shown in Figure 5b, upon immediate addition of DMEM (DMEM-0), all of the polyplexes increased in size (between 250 and 450 nm) possibly due to particle swelling and/or neutralization of the surface charge and some colloidal aggregation. Polyplexes formed with **9a** and **9b** continued to aggregate rapidly with time, and a bimodal distribution of polyplexes was observed that contained a mixture of very large aggregates (over 3 μm) with some smaller complexes. Conversely, **9c** polyplexes revealed a different trend and aggregated much slower after the initial addition of DMEM containing serum. After 60 min of DMEM exposure, the average **9c** polyplex size remained about 350 nm. These results indicate that the amine number between the trehalose and triazole moieties affects the stability of polyplexes in biological media containing serum. Polymer **9c** contains a longer oligoamine block between the triazoles, and the gel shift and EB exclusion assays imply that this particular structure binds pDNA with higher affinity. Moreover, the TEM results demonstrate that this structure condenses pDNA into smaller and more spherical polyplexes. Theoretical studies have shown that polycations with lower charge density (such as **9a** and **9b**) tend to form looser complexes with polyanions.[18] This characteristic could then allow partial disassembly of **9a** and **9b** polyplexes to occur under physiological salt and serum conditions, providing a higher colloidal surface area and promoting polyplex−polyplex and polyplex−serum aggregation.

Conventionally, large steric barriers of hydrophilic polyoxomers with molecular weights between 2.5 and 5.0 kDa are commonly grafted on the periphery of nanoparticles to prohibit flocculation in biological media.[2,20,21,46] These materials successfully prevent aggregation through steric stabilization, which prevents polyplex−polyplex flocculation and nonspecific adsorption of biological proteins (i.e., serum), which increases circulation times in vivo.[2,21,46,47] This property can also adversely affect interaction of these polyplexes with the cell surface, thus negatively impacting cellular uptake. The decreased aggregation behavior of **9c** polyplexes in biological media containing serum (as compared to **9a** and **9b** polyplexes), as well as its stronger binding characteristics, is intriguing. The combination of these observations suggests that **9c** may form complexes with pDNA that expose more of a hydrophilic trehalose layer on the polyplex surface, which could discourage serum-mediated aggregation. This could be promoted by the longer oligoamine moieties between the disaccharide groups. In support of this hypothesis, it is well known that trehalose prohibits protein and lipid

(46) (a) Ogris, M.; Brunner, S.; Schuller, R.; Kircheis, R.; Wagner, E. *Gene Ther.* **1999**, *6*, 595−605. (b) Hwang Pun, S.; Davis, M. E. *Bioconjugate Chem.* **2002**, *13*, 630−639.
(47) Otsuka, H.; Nagasaki, Y.; Kataoka, K. *Curr. Opin. Colloid Interface Sci.* **2001**, *6*, 3−10.

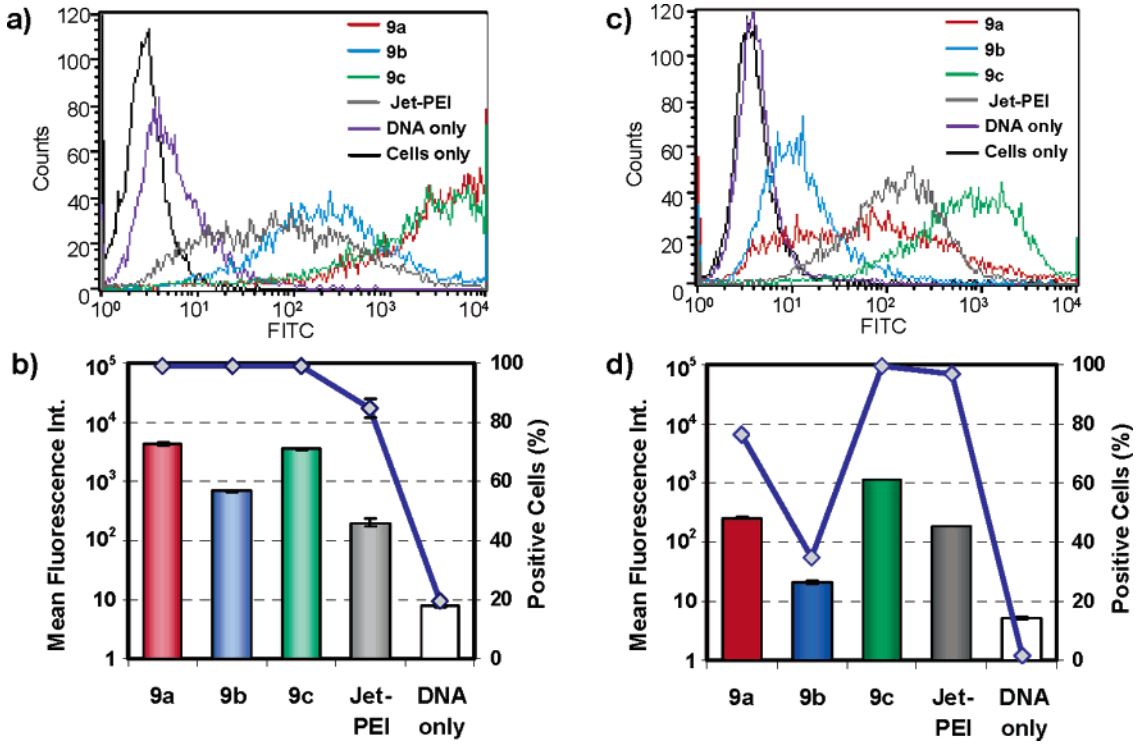

Figure 6. Cellular uptake of fluorescein (FITC)-labeled pDNA complexed with **9a**, **9b**, and **9c** at an N/P = 7 and Jet-PEI at N/P = 5. (a) Flow histogram of HeLa cells after transfection in serum-free Opti-MEM. (b) Relative amount of FITC−pDNA per cell as the mean fluorescence intensity (bars) and the percentage of cells positive for FITC−pDNA (line) after transfection in Opti-MEM. (c) Flow histogram of HeLa cells after transfection in DMEM with 10% serum. (d) Relative amount of FITC−pDNA per cell as the mean fluorescence intensity (bars) and the percentage of cells positive for FITC−pDNA (line) after transfection in DMEM. Each data point represents the mean +/− standard deviation of three replicates.

aggregation in biological systems upon dehydration and freezing.[34] In addition, Fidy et al. have revealed that the presence of free trehalose in solution can prevent aggregation of human serum albumin with neutral and charged liposomes.[48] They attribute this finding to the large hydrated volume of this carbohydrate (2.5 times that of sucrose) and the fact that this sugar may associate with the liposome surface and sterically prohibit liposome−serum interactions. Trehalose has also been found to prohibit polyglutamine-mediated protein aggregation and is therefore being researched as a possible treatment option for Huntington's disease.[49] Further studies aimed at understanding the binding characteristics and stability of **9c** polyplexes in the presence of serum are in progress.

Cellular Delivery and Toxicity Studies. The delivery of nucleic acids mediated by polymeric vectors involves a complex pathway that requires the colloidal polyplexes to bypass numerous destructive obstacles while retaining the ability to release their genetic payload within the proper cellular location.[2,5,14,50] Polymeric delivery agents have proven to be an effective means to transfect cells in vitro in the absence of serum. However, attempts to develop synthetic systems that yield high delivery efficacy in the presence of serum have not been particularly successful.[5,36] For this reason, the design of novel materials that stabilize polyplexes from aggregation in the presence of serum and still promote effective delivery of their payload into targeted cells is highly sought after. Thus, fine-tuning the polymer chemistry and physical properties of these systems and understanding the structure−property relationships are of the utmost importance to increase their biological efficacy.

The new glycopolymers formed via click polymerization were examined for their ability to deliver FITC-labeled pDNA with HeLa (human adenocarcinoma) cells. This technique determines the percentage of cells positive for FITC-labeled pDNA (Figure 6, line) and is therefore a direct determination of pDNA delivery efficiency as a function of polymer structure. Also, the relative amount of pDNA delivered per cell can be qualitatively assessed based on the average fluorescence intensity (Figure 6, bars) as determined via flow cytometry analysis. This experiment was performed under two conditions: (i) in serum-free media (Opti-MEM) and (ii) in the presence of media containing 10% serum (DMEM). As shown in Figure 6, all of the glycopolymers delivered pDNA into HeLa cells. As shown in Figure 6a and 6b, polymers **9a**−**9c** all transfected about 99% of HeLa cells in Opti-MEM. These results were compared to our controls of pDNA only and Jet-PEI, where a lower percentage of cells were transfected under these conditions (20% and 87% of HeLa cells, respectively). The vectors, however, revealed differences in the average amount of pDNA that was transfected into each cell, where polymers **9a** and **9c** appeared to be the most effective systems in Opti-MEM, where the average fluorescence intensity per cell was about an order of magnitude greater than the cells transfected with Jet-PEI and **9b**.

In DMEM with 10% serum, a larger difference in the transfection efficiency data was noticed (Figure 6c and 6d). Polymer **9c** was clearly the most effective vector, and it was interesting to find that **9c** still transfected 99% of HeLa cells and revealed the highest mean fluorescence intensity (more

(48) Bardos-Nagy, I.; Galantai, R.; Laberge, M.; Fidy, J. *Langmuir* **2003**, *19*, 146−153.
(49) Tanaka, M.; Machida, Y.; Niu, S.; Ikeda, T.; Jana, N. R.; Doi, H.; Masaru, K.; Nekooki, M.; Nobuyuki, N. *Nat. Med.* **2004**, *10*, 148−154.
(50) Nishikawa, M.; Hashida, M. *Biol. Pharm. Bull.* **2002**, *25*, 275−283.

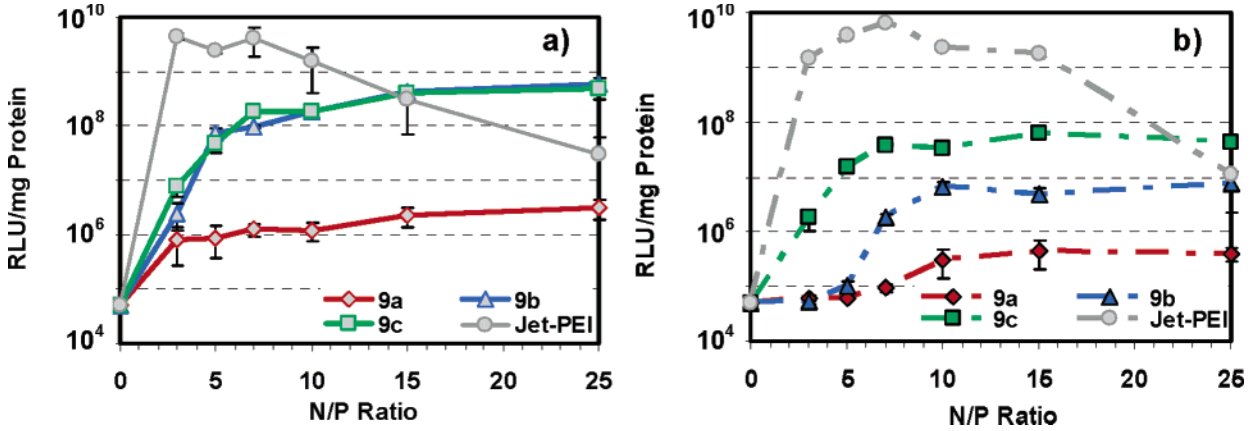

Figure 7. Luciferase reporter gene expression with **9a**, **9b**, **9c**, and Jet-PEI polyplexes formed at N/P ratios of 0 (DNA only), 3, 5, 7, 10, 15, and 25. Data are reported as relative light units (RLU)/mg protein as the mean +/− standard deviation of three replicates. (a) Gene delivery in serum-free Opti-MEM. (b) Gene delivery in DMEM containing 10% serum.

pDNA per cell) of all of the vectors. This result is likely related to the high pDNA-binding affinity and the slower aggregation of **9c** polyplexes in DMEM with serum. Transfection of pDNA with **9a** and **9b** was clearly impacted by the presence of serum, where only 76% and 35% of cells were positive for FITC−pDNA with these systems, and the mean fluorescence intensity was similarly low. It is interesting to note that the percentage of cells positive for FITC−pDNA with Jet-PEI was slightly higher in the presence of DMEM than in Opti-MEM. This result is likely related to an overall increase in the viability of cells exposed to this vector in DMEM (vide infra).

Luciferase reporter gene delivery experiments were also performed with HeLa cells to examine the gene expression profiles of polyplexes formed with these systems in serum-free Opti-MEM and DMEM containing 10% serum. In the absence of serum (Figure 7a), polymers **9b** and **9c** were equivalent in their luciferase expression profiles. With these systems, the observed gene expression increased steadily as the N/P ratio increased from 3 to 10 and then leveled out at N/P = 15. Polymer **9a** revealed very low gene expression in Opti-MEM that did not increase appreciably with the N/P ratio. When these data were compared to the cellular uptake data (Figure 6a and 6b), it was noticed that although **9a** transfected about 99% of cells and delivered a relatively high amount of pDNA into each cell (similar to **9c**), the gene expression profile is very low. This result may indicate that endosomal release of **9a** polyplexes (and subsequent trafficking to the nucleus for expression) is a major limiting factor with this vector. It is interesting to note that an opposite trend was found with **9b** and the control, Jet-PEI, where both vectors delivered a relatively low average amount of pDNA per cell yet the gene expression was high. Vector **9c** consistently had high cellular uptake and gene expression profiles. The fact that **9c** yielded higher cellular uptake but lower gene expression than Jet-PEI suggests that the endosomal barrier may be a limiting factor for this vector as well.

In the presence of serum, polyplexes typically have lower delivery efficiency due to interaction and aggregation of these complexes with serum proteins. As shown in Figure 6b, the gene expression results in the presence of serum were significantly different than that observed in Opti-MEM. Polyplexes formed with **9a** were again the least effective, which could be related to the aggregation behavior of this system with serum proteins and lack of endosomal escape of these complexes (and subsequent degradation). Unlike the data obtained in Opti-MEM, it was observed that **9b** yielded lower gene expression in the presence of serum than **9c**. The combination of the polyplex stability, cellular uptake and gene expression data suggests that **9b** rapidly aggregates with serum proteins, which severely limits the transfection ability of this vector. In contrast, polyplexes formed with **9c** clearly revealed a higher gene expression profile, which is likely a result of the low aggregation of these polyplexes in DMEM. It was also revealed that polyplexes formed with **9c** were effective at lower N/P ratios of 5 and 7, which could be related to the high binding affinity of this polymer with pDNA (Figure 4). Jet-PEI was used as a positive control in these studies and shows that this vector has a very high gene expression profile in both Opti-MEM and DMEM even though the cellular uptake profiles are lower than **9a** and **9c**. These data indicate that the number of amines within the polymer repeat unit significantly affects the gene expression within HeLa cells. Considering the differences between the cellular uptake (Figure 6) and gene expression data (Figure 7), the endosomal escape of these polyplexes could be a limiting factor in promoting very high gene expression. It appears that as the number of amines increases (**9a** < **9b** < **9c** < Jet-PEI), the gene expression increases (and possibly the ability to escape the endosomes).

Understanding how the chemical structure of the polymers affects cytotoxicity is extremely important to determining the promise of the systems for in vivo use; thus, the cytotoxicity was examined at all N/P ratios of delivery. The results of this assay at N/P ratios of 7 and 15 in both Opti-MEM and DMEM are shown in Figure 8. The polyplexes formed with **9a**, **9b**, and **9c** generally displayed higher toxicity in Opti-MEM than in DMEM. In Opti-MEM, at N/P = 7 (Figure 8a), all of the systems displayed a low level of toxicity, where cell viability values ranged between 70 and 80%. At N/P = 15, there was greater diversity in the values observed, where **9a** and **9b** yielded lower toxicity (about 80% cell survival); however, **9c**, revealed elevated toxicity, with cell viability values of 50%. The lower viability value noticed with **9c** at N/P = 15 ratio was most likely due to the higher amine density along the polymer backbone. The cell survival profiles with vectors **9a**−**9c** were much higher than Jet-PEI, which revealed only 18% and 10% cell survival rates at N/P ratios of 7 and 15, respectively. Increasing the number of amines can strengthen the interaction of the polymers

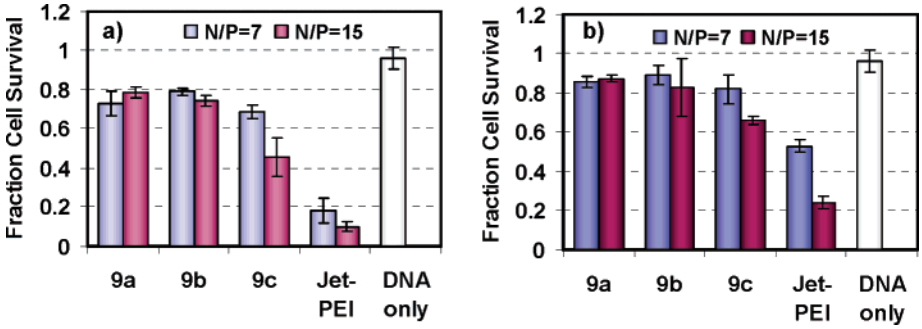

Figure 8. Toxicity of pDNA only and polyplexes formed with **9a**, **9b**, **9c**, and Jet-PEI at N/P ratios of 7 and 15 displayed as the fraction of HeLa cell survival. The data are reported as a mean +/− standard deviation of three replicates, and the values have been normalized to untransfected cells (cell survival = 1.0). (a) Fraction of cell survival in serum-free Opti-MEM. (b) Fraction of cell survival in DMEM containing 10% serum.

with cellular membranes and can inhibit proper membrane function. It should be noted that the glycopolymers presented here have many similarities in structure to aminoglycoside antibiotics. Aminoglycosides are known to interact strongly with anionic phospholipids and can prohibit intracellular vesicle fusion, which has been proposed to be a main cause of their toxicity.[51]

In serum, the toxicity profiles were significantly lower, where at N/P = 7, the glycopolymers all yielded cell viability values between 80 and 90%. At N/P = 15, cell viability was also higher than the Opti-MEM results, where more than 80% of the cells survived with **9a** and **9b** polyplexes and about 70% cell survival was noticed with **9c**. The lower viability value for **9c** at this high N/P ratio was not a concern because greater than 80% cell viability was revealed at N/P = 7, where close to maximum gene expression values were observed. Again, Jet-PEI revealed higher toxicity in DMEM (only about 50 and 25% of the cells survived at N/P ratios of 7 and 15, respectively).

Conclusion

In conclusion, a novel series of glycopolymers have been synthesized through click polymerization. This transformation allowed for efficient carbohydrate and oligoamine monomer coupling, yielding degrees of polymerization almost 5 times that obtained via aminolysis polycondensation used to synthesize analogous poly(glycoamidoamine)s.[3,4,16] The results presented herein demonstrate that the trehalose click polymers designed in this study are very effective nucleic acid carriers in both the absence and presence of serum. Vector **9c** revealed exceptionally stable polyplex formation, high cellular delivery, and relatively low toxicity, particularly in the presence of serum at low N/P ratios. This discovery is of great importance for developing polymeric nucleic acid delivery vehicles for in vivo applications. The ability to utilize the click reaction to synthesize biocompatible materials that bind and compact DNA at low N/P ratios is important for assembling polyplexes that evade humoral and toxic responses associated with the large excess of material that is commonly needed to promote high delivery efficiency in the presence of serum. Also, the use of a trehalose moiety within the polymer repeat unit may promote serum stability without grafting on large poly(ethylene glycol) chains to the polymer backbone. This unique property may allow researchers in this area to design novel delivery vehicles that are stable, yet still highly effective under the harsh physiological conditions encountered during systemic delivery. This means of stabilizing nanoparticles from serum aggregation may be extended to other colloidal nanoparticle systems. Studies aimed at understanding why **9c** appears to reduce serum-mediated polyplex aggregation as well as deciphering the cellular barriers involved in achieving maximum gene expression with these systems will be presented in due course.

Acknowledgment. We sincerely thank Dr. Valery Fokin for helpful discussions about the click reaction. Financial support was provided by the NIH (R21EB003938-01), the NSF CAREER (CHE-0449774), and the Beckman Young Investigators programs.

Supporting Information Available: Experimental details of the synthesis and characterization of **2**−**4**, **6a**−**6c**, **7a**−**7c**, **8a**−**8c**, and **9a**−**9c** and details of the electrophoresis, ethidium bromide exclusion assays, TEM, dynamic light scattering, cell culture, flow cytometry, reporter gene, and viability assays. This material is available free of charge via the Internet at http://pubs.acs.org.

JA0585580

(51) van Bambeke, F.; Mingeot-Leclercq, M.-P.; Brasseur, R.; Tulkens, P. M.; Schanck, A. *Chem. Phys. Lipids* **1996**, *79*, 123−135.